16TH EUROPEAN CONFERENCE ON EARTHQUAKE ENGINEERING THESSALONIKI 18 - 21 JUNE 2018

NON-STRUCTURAL RISK EVALUATION: EXPERIENCES FROM PILOT AREAS OF THE KNOWRISK PROJECT

Raffaele AZZARO[1], Salvatore D'AMICO[1], Horst LANGER[1], Fabrizio MERONI[1], Thea SQUARCINA[1], Giuseppina TUSA[1], Tiziana TUVE'[1], Rajesh RUPHAKETI[2], Simon OLAFSSON[2], Bjarni BESSASON[2], Carlos Sousa OLIVEIRA[3], Mónica Amaral FERREIRA[3], Francisco MOTA DE SÁ[3], Mario LOPES[3]

ABSTRACT

This paper presents a multidisciplinary approach to quantify seismic hazard and ground motion intensity parameters for non-structural seismic risk evaluation. In the framework of the European KnowRISK Project, three pilot areas were selected for testing different methodological approaches aimed at evaluating elements and measures to reduce seismic risk coming along with the failure of non-structural elements. At Mt. Etna, Italy, instrumental and historical macroseismic data are used to generate ground motion time series for different scenario events. Risk maps for non-structural damage are generated by using building vulnerability from census data and a damage model based on fragility curves; interstory drift spectra have been also calculated for a representative test site. In South Iceland, scenarios are defined basing on the June 2000 seismic sequence, which provided strong-motion data at several locations. The recorded data and other parameters of the source are used to perform finite-fault simulations of ground motion at different locations in the area and then to calculate interstory drift spectra. In Portugal a scenario referring to the Lower Tagus Valley was selected and finite-fault simulations for the nearby city of Lisbon were performed.

Keywords: KnowRisk Project; ground motion parameters; drift spectra; non-structural element; seismic risk.

1. INTRODUCTION

Quantification of risk for non-structural damage is more challenging than that for structural damage due to two main reasons. Firstly, the return period of earthquakes to be relevant for non-structural damage is not well defined by regulatory codes, although it is generally recognized to be short since this kind of effects derive both from the near-field moderate earthquakes and far-field stronger events. Secondly, non-structural damage is related to parameters of ground motion which are different than those conventionally used for structural design and capacity evaluation.
The KnowRISK project focuses, in Task B, at defining the seismic scenarios that are critical for non-structural damage, identifying relevant ground motion intensity parameters and, finally, producing risk maps. The different approaches adopted in the pilot areas – namely Mt. Etna volcano in Italy, South Iceland, and Lisbon in Portugal – are based on updated seismic hazard maps and earthquake scenarios. The ground motion parameters have been referred to two different EC8 soil profiles and then used to calculate drift spectra, allowing the identification of simple schemes for the assessment of non-structural vulnerability. Final risk maps have been obtained by deterministic or probabilistic approaches, considering census data of building vulnerability, damage models and fragility curves.

[1]Istituto Nazionale di Geofisica e Vulcanologia, Italy, raffaele.azzaro@ingv.it
[2]Earthquake Engineering Research Centre, Selfoss, Iceland, rajesh@hi.is
[3]Instituto Superior Técnico, Dept of Civil Engineering, Architecture and Georesources, CEris, Lisbon, Portugal, csoliv@civil.ist.utl.pt

2. DEFINITION OF SEISMIC SCENARIOS

The seismic scenarios for the assessment of non-structural damage have been defined according to the nature of seismicity in the pilot areas of the three participating countries. At Etna volcano, Italy, the very shallow, recurrent volcano-tectonic earthquakes represent the main source of non-structural damage, while the crustal events control the seismic scenarios in both far- and near-field, the main epicentres being located along the Atlantic Ocean plate boundaries and the Lower Tagus Valley. In methodological terms, the hazard analysis considers macroseismic data or ground motion parameters instrumentally derived or calculated by means of synthetic simulations. In this way we identified the areas that are mostly exposed to intensities/shaking typically representative of non-structural damage.

2.1 Mt. Etna volcano, Italy

The definition of seismic scenarios has been tackled in terms of macroseismic intensity, adopting the probabilistic approach based on the Bayesian statistics to calculate the probabilistic distribution of the intensity expected at a given site conditioned on the epicentral intensity of the earthquake and the distance from the epicentre (Zonno et al., 2009). In the EMS scale (Grünthal, 1998), non-structural damage (grades 1, 2 and 3) is confined mainly between degrees VI and the VII, while starting from degree VIII the structural component of damage becomes predominant (grades 3, 4 and 5). For the purposes of the KnowRISK project, we therefore focused on mapping occurrence probabilities relevant for intensities VI and VII. The seismic hazard map (Azzaro et al., 2016) shows that, for short exposure times (e.g. 30 years), the eastern flank of Etna presents a probability greater than 50% to suffer extensive non-structural damage related with degree VII EMS (Fig. 1a), while the probability increases to 80% if referred to slight non-structural damage determined by degree VI EMS.

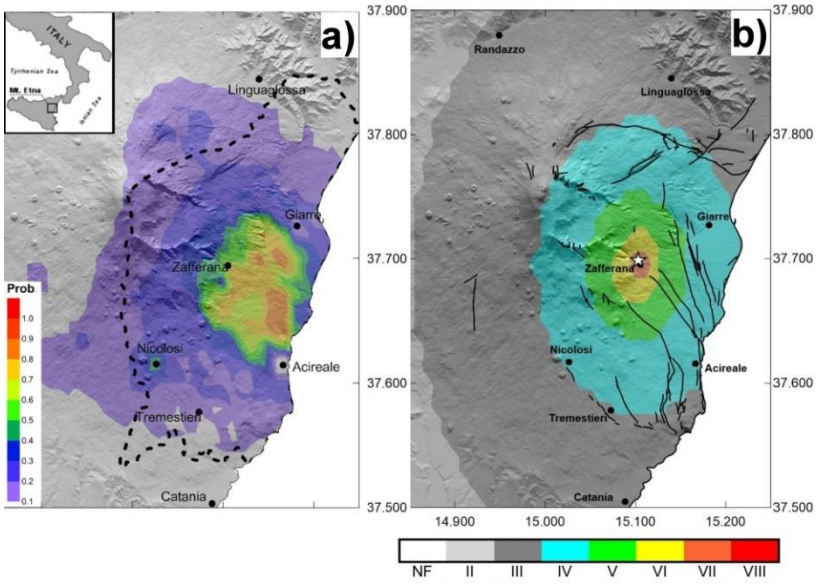

Figure 1. a) Distribution of occurrence probabilities for degree VII EMS in 30 years; b) Probabilistic seismic scenario calculated for the October 19th, 1984 earthquake (epicentral intensity I_0 = VII EMS, M_w 4.2).

We selected the town of Zafferana as test site, since the high probability to be struck with an intensity at least of degree VII EMS in 30 years as well as the availability of census data on building stock. The hazard deaggregation analysis referred to this locality, enabled us defining the "design earthquake", i.e. a class of distance/magnitude bins of events which occurred in the past (Albarello, 2012) and most contributed to the hazard of that site. Results show that hazard associated with intensity VII is due to small size earthquakes – M_w ranging from 4.0 to 4.3 – with epicentres close to this site (within 6 km). Conversely, stronger earthquakes occurring farther away less contribute to the hazard. This conclusion and the analysis of the seismic history of the site (see catalogue CMTE, 2017) suggested us to select as input for the seismic scenario the October 19th, 1984 M_w 4.2 earthquake.

Figure 1b shows the intensities used for the scenario, calculated according to the method reported in Azzaro et al. (2013) and Rotondi et al. (2016). Note the strong attenuation of intensity in short distances and non-structural damage related with degrees VII and VI around the test-site (Zafferana).

2.2 South Iceland Seismic Zone

Seismicity of Iceland is described in detail in D'Amico et al. (2016a). The study area of this project is the SISZ and Reykjavik. After the south Iceland earthquakes of 2000, ground motion data required for calibration of empirical ground-motion prediction equations (GMPEs) in Iceland became available and more detailed studies on probabilistic seismic hazard assessment (PSHA) using instrumental ground-motion measures followed. Solnes et al. (2004) used a simulated parametric catalogue and a locally calibrated GMPE based on Brune's source spectrum to compute 475-year return period hazard map for horizontal PGA (Fig. 2). More recently, new hazard estimates for Iceland have been provided for several return periods in the EU project SHARE (http://www.share-eu.org/node/6, Giardini et al., 2013; Woessner et al., 2015). The map for PGA with 10 % probability of exceedance in 50 years (Fig. 2) shows significant differences to the map of Solnes et al. (2004), due to the different earthquake catalogues, source models and attenuation relationships considered in the two studies.

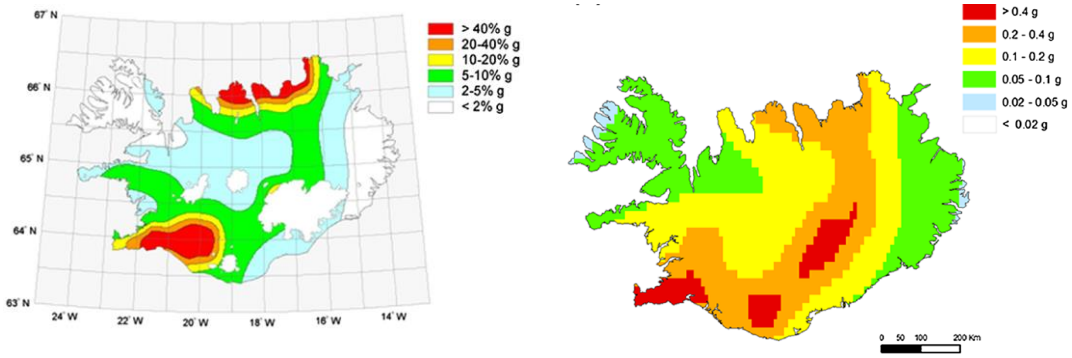

Figure 2. Probabilistic seismic hazard map of Iceland from Solnes et al. (2004) (left) and from SHARE project (http://www.efehr.org:8080/jetspeed/portal/hazard.psml) (right).

Modern design codes are lacking in providing clear guidelines for limiting damage caused by building contents. One of the main challenges is that the corresponding hazard scenario is poorly defined. The selection of an appropriate scenario partly depends on building practice. For example, wind load requirements in Iceland are so stringent that most of the buildings safely withstand very high level of ground acceleration during earthquake without much structural damage. The experience from the three recent earthquakes, the two in June 2000 and one in May 2008 have shown that, even in areas which experienced ground shaking twice the level of prevalent seismic design requirements, structural damage was negligible compared to non-structural damage (Bessason and Bjarnason, 2016; Rupakhety et al., 2016). However, significant non-structural damage was suffered. In addition, damaging earthquakes in SISZ happen in sequences and are often of similar size (M_w 6.3-6.5), although larger earthquakes can be expected in the eastern part of SISZ. In this context, for the SISZ area, a suitable scenario earthquake is the one that corresponds to life safety performance level. In other words, deaggregation of 475-year hazard level can shed light on the most relevant scenario. De-aggregation of seismic hazard in past studies (Solnes et al., 2004, D'Amico et al., 2016a) shows that earthquakes of M_w 6.3 within 5 to 15 km epicentral distance are the most significant contributors of 475-year return period hazard in SISZ.

2.3 Lisbon, Portugal

Portugal presents a more complex seismicity pattern characterized by: i) inter-plate seismic sources located offshore at the junction of the Eurasian and African Plates, responsible for the 1755 Lisbon M 8.5 earthquake and the 1969 Gorringe Bank M 7.9 earthquake; ii) intra-plate onshore events, with higher frequency contents (Fig. 3).

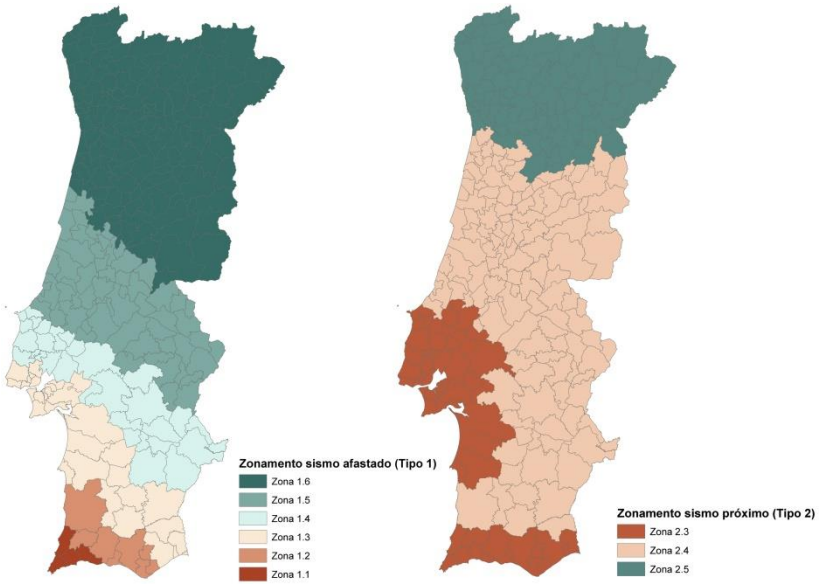

Figure 3. Eurocode (EC-8) zones (Portuguese National Annex, 2010) for inter-plate (left) and intra-plate (right) seismicity.

The seismogenic source capable of producing moderate to large earthquakes in Portugal and particularly the capital city of Lisbon, is the Lower Tagus Valley Fault (Fig. 4a), extending as far as Lisbon. Two main earthquakes occurring in 1344 and 1531 (M 7.0), caused severe damage in the region and Lisbon. In 1909, a M 6.3 earthquake caused 54 victims and destroyed several small towns located along the Tagus Valley (Teves-Costa et al., 2000). Due to the high concentration of population (ca. 3 million of inhabitants), this region is considered as a high seismic risk zone.
According with Vilanova and Fonseca (2004), a magnitude 6.5-7.0 with a return period of 200 years can be expected for the Lower Tagus Valley fault. In an exposure period of 95 years, accelerations in Lisbon can reach the value of 1.1 m/s^2 and could affect more than 3 million people living in this area. Considering the attenuation law for earthquakes Type II (Carvalho, 2008), such a seismic input can be simulated by an M 6.5 located at about 15 km NE of Lisbon. Therefore, we assume it as the earthquake scenario (Fig. 4b).

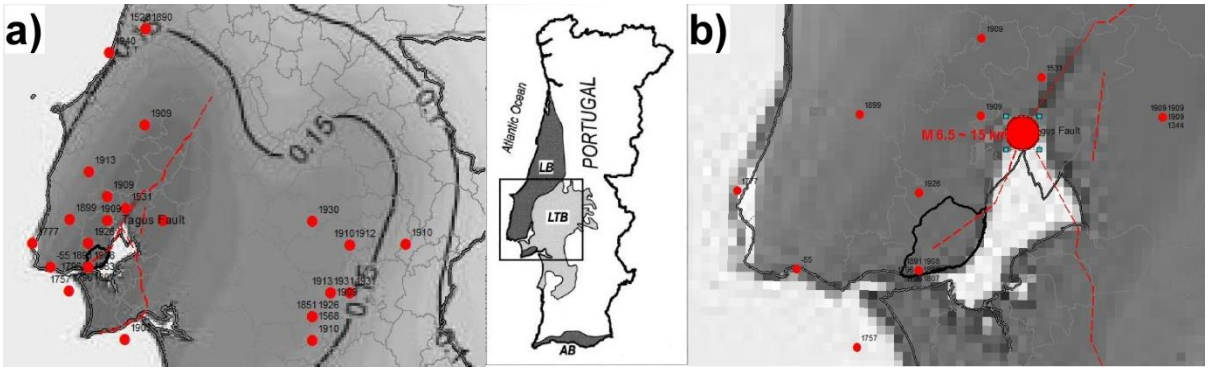

Figure 4. a) Lower Tagus Valley fault (LTV, red dashed line); historic earthquakes and hazard map proposed by Vilanova and Fonseca (2004) for earthquakes Type II. Frame, LTB: Lower Tagus Basin; b) M 6.5 event (TR 95 years) and epicenter of the Lisbon earthquake scenario.

For simulating the scenario, information from the Building Census of 2011 was employed, thus disregarding public infrastructures and considering only commercial or industrial buildings. In 2011, the Lisbon building stock consisted of 52,496 residential buildings, housing 323,076 dwellings, organized in 69 different typologies: 49 masonry typologies representing about 53% of the whole building stock, and 20 reinforced concrete (RC) typologies for the remaining 47% of buildings. For

each one of them, capacity curves were recently reviewed in Mota de Sá (2016). The seismic risk assessment of Lisbon was carried out also using the QuakeIST earthquake simulator (Mota de Sá et al., 2016).

Table 1. Simulation results: epicenter in the LTV fault, 15 km from Lisbon, with an average PGA 1.12 m/s^2.

Typology	**N° buildings**	**%**	**D0**	**D1**	**D2**	**D3**	**D4-D5**
Masonry	29923	57%	299	1496	4788	9874	13465
			1%	5%	16%	33%	45%
RC	22573	43%	7449	4515	3160	3612	3837
			33%	20%	14%	16%	17%

Looking at Table 1, we observe: i) the EC-8 objective of "Damage Limitation" (non-structural losses) is violated in 58% -74% of all buildings (damage grades 2- moderate to extensive damage-damage grade 3); ii) EC-8 violation of the objective of "Damage Limitation" in 78%-95% in masonry buildings (in accordance to CENSUS 2011(INE, 2011) representing about 57% of the whole building stock in Lisbon, and 32%-47% of RC buildings (representative of 43% of the whole building stock).

3. IDENTIFICATION OF GROUND MOTION INTENSITY PARAMETERS

This problem was analysed considering three main directions. The first is related to the evaluation of intensity measures that are more structure-specific than peak ground motion or response spectra based parameters. This relates to the evaluation of inter-story drift spectra and floor acceleration spectra. The second direction is related to experimental investigations, which include tests of shaking table as well. The third direction is through numerical modelling using the formulation of rocking of rigid blocks.

3.1 Mt. Etna volcano, Italy

In the scenario based approach we attempt to bypass the lack of instrumental strong motion records developing physical models and generating synthetic data. Existing weak motion recordings have been used to verify the validity of physical concepts at the base of the simulations (see Langer et al., 2016). As the KnowRisk project focuses on non-structural damage, we consider - besides peak amplitudes and the response of a damped SDOF system – the so called drift spectra, which may provide a better understanding of those phenomena. We demonstrate the design of the scenario considering the village of Zafferana, repeatedly hit by various damaging events. This site is typical for the eastern flank of the volcano, where about 400,000 people are living an area of approximately 510 square kilometers including 28 municipalities. We may identify two relevant scenarios: i) seismic events with Zafferana falling in the epicenter zone and ii) events occurring at some distance (5-10 km). Synthetic simulations of ground motion scenarios are based on the code EXSIM (see Boore, 2009) with slight modifications (Langer et al., 2016). Simulations carried out regard an earthquakes M 4.2 close to the site and a further one, M 5.0 at a distance of 7 km: parameters were chosen following Langer at al. (2016). Two types of site were considered. For the hardrock site no specific amplification factors were applied. Besides we also considered site amplifications for a D-type soil applying the functions given in Scarfì et al (2016). Simulated ground motion parameters for both scenarios are reported in Table 2; Fig. 5 gives sample of response spectra.

Table 2. Ground motion parameters for the two scenarios using a factor of 0.9 for the partition between the two horizontal components. PGA, peak ground acceleration; PGV, peak ground velocity; IH, Housner Intensity; Ieq, "equivalent" macroseismic intensity estimated through the empirical relationship by Chiauzzi et al. (2012).

Event M= 4.2, epicenter	**PGA (gal)**	**PGV (cm/s)**	**IH (cm) (Ieq)**
Site H	19.6	1.7	11 (5.5)

Site D	130	13	67 (7.6)
Event M= 5, dist = 7 km	**PGA (gal)**	**PGV (cm/s)**	**IH (cm) (Ieq)**
Site H	14	1.4	11 (5.5)
Site D	77	11	73 (7.7)

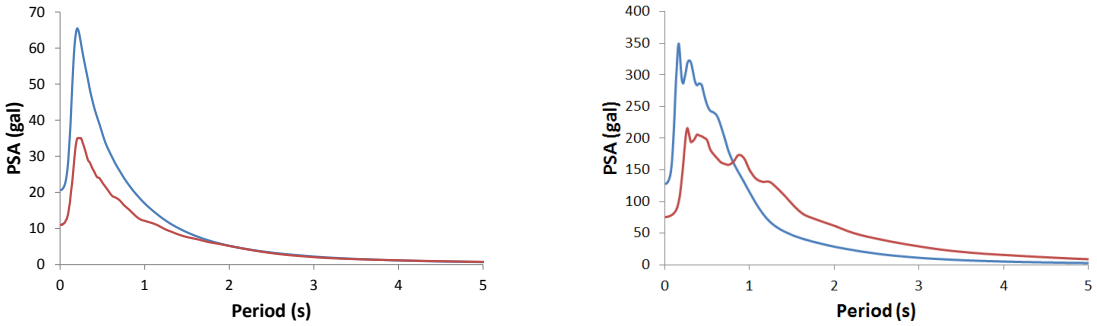

Figure 5. Left: response spectra for "Hardrock". Right: response spectra for "Soft Soil". Blue line: M 4.2 at the epicenter; red line: M 5 at a distance=7 km.

The inter-story drift ratio is the response parameter best correlated with damage in buildings (Miranda and Akkar, 2006). It is also a relevant parameter for all items fixed to the walls, e. g., furniture, tiles, as well as lifelines, such as gas and water conduits. Contrary to classical response spectra, the inter-story drift ratio is based on a model that consists of a combination of a flexural beam and a shear beam. The lateral stiffness ratio, α is a dimensionless parameter that controls the degree of participation of overall flexural and overall shear deformations in the continuous model, thus controlling the lateral deflected shape of the model. A value of α equal to zero represents a pure flexural model and a value equal to ∞ corresponds to a pure shear model. Critical parameters in the model are α, the height H (and its relation to the natural period of the building), and the damping. We have been using a constant damping of 5%. From a seismological point of view, geological condition of the sites is among the most critical issues. Setting for the moment the parameter α=20 and using a relation *H/m=10 T/s*, we obtain the drift spectra for the test site as shown in Fig. 6. For the hardrock site no specific amplification factors were applied. Besides, we also considered site amplifications for a D-type soil applying the functions given in Scarfì et al. (2016).

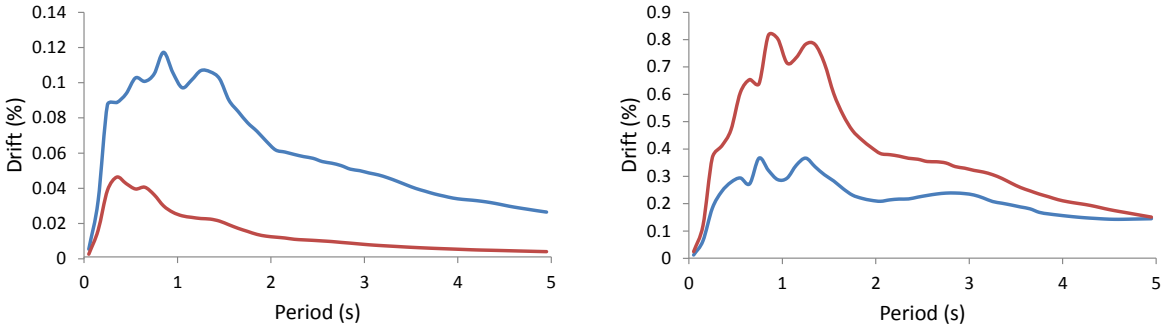

Figure 6. Left: drift spectra (average over 12 azimuth directions) for "Hardrock". Right: drift spectra for "Soft Soil". Red line: M 4.2 at the epicenter; blue line: M 5.0 at a distance = 7 km.

Peak ground motion parameters, response spectra and drift spectra underscore the relevance of geological site conditions. In the case of soft soil we observe critical values for the case of M=4.2 earthquake with the site falling the epicenter area. The latter affects in particular the higher frequencies (>1 Hz), which stand for smaller buildings (H<10 m). For the larger event, peak ground acceleration and spectral values are lower in the high frequency range than in the case before. The average drift

spectra are below the critical value of 0.5% reported in the EC08. Note, however, that standard deviations of the values shown in Fig. 4 amount to 20-30% for the M5.0 scenario, and up to 60% in the M 4.2 case. That means that there is a fair possibility of drift reaching critical values (in the sense of EC8) for both scenarios assuming soft soil conditions. On the other hand, non-structural components may be damaged at inter-story drifts well below the 0.5% of the EC8 brittle attach components. Cracking on masonry walls and infills is typically triggered at ratios of ca. 0.15% - 0.2%.

3.2 South Iceland Seismic Zone

Although the main study area in Iceland is the SISZ, Reykjavik area was also considered due to its large population density. The following two scenarios were considered: i) Reykjavik: M_w 6.0 event with epicentral distance of 31 km; ii) Selfoss: M_w 6.3 event with epicentral distance of 9 km.
The ground motion time series corresponding to these scenarios are obtained from recorded data of past earthquakes. The nature of ground motion at these two scenarios is very different. The motion in Reykjavik is of low amplitude and more broadband in nature, while in Selfoss it is of much larger amplitude and contains narrow-band pulses (more dominant in velocity time series) typical of near-fault ground motions. The corresponding drift spectra are shown in Fig. 7, where the Eurocode 8 limits for different components are shown with horizontal dashed lines. For example, non-attached components have a limit of 1% interstory drift. The drift spectra are shown for three different values of the parameter. The effect of this parameter in the scenarios seems to be not very significant. It should be pointed out that most buildings in Iceland contain shear walls and moment resisting frames are rare. Therefore, the most relevant spectra for this case study correspond to the blue curves in Fig. 7. The drift spectra in Reykjavik is much smaller than that in Selfoss, which is expected due to the much smaller amplitude of ground shaking in Reykjavik. The drift spectra in Reykjavik are lower than the EC8 limits. This, however, should not be interpreted as a general conclusion, because the results being presented here correspond to one typical scenario, which contributes most to the 475 year return period hazard. Closer earthquake scenarios may produce higher drift demands on buildings in Reykjavik. The scenario in Selfoss is quite different, as it lies very close to the SISZ. In this case, the drift spectra have a peak around a period of 0.8s, which can be attributed to the long-period velocity pulse in the ground motion used for this scenario. Buildings with fundamental period close to 0.8 exceed all levels of limiting drifts specified in EC8. This, however, is not a major concern, because many buildings in Selfoss are stiff and only 1-3 story tall, with fundamental period generally less than 0.2s. Therefore, the critical case for Selfoss seems to be brittle components attached to the structure. Also, note that these spectra do not accurately represent potential damage to freestanding contents.

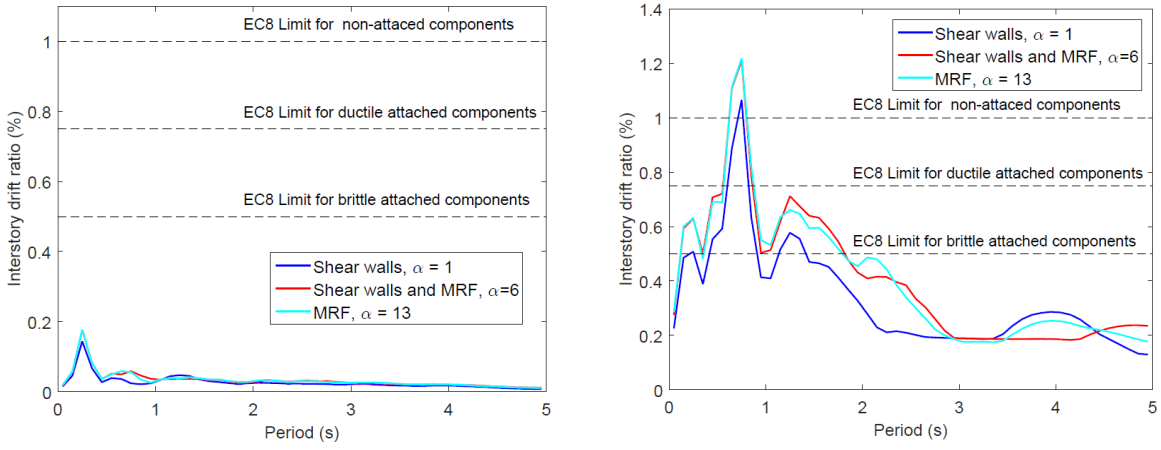

Figure 7. Drift spectra in Reykjavik (left) and Selfoss (right).

4. MAPPING THE RISK

Risk was evaluated at the study areas using different approaches. The use of different approaches was

necessitated by local constraints such as availability of data, nature of hazard, vulnerability of structures, etc.

4.1 Mt. Etna volcano, Italy

The study of the seismic risk of an urban region follows two steps: (i) exposure geo-referenced inventory and vulnerability classification of assets at risk; (ii) vulnerability characterization according to damage models. Here, damage models are selected according to the macroseismic evaluation of the seismic hazard provided before, so a method for the vulnerability assessment has been adopted. The damage model proposed by Lagomarsino and Giovinazzi (2006) and revised in Bernardini et al., (2007), was successfully applied in previous Portuguese and Italian seismic risk studies (Sousa, 2006; Sousa, 2008; D'Amico, 2016b). This model classifies the building stock according to the vulnerability table of the EMS, and predicts damage distributions conditioned by an intensity level for each damage grade of the scale. Thus, the seismic vulnerability of the elements at risk that belong to a given building typology (i.e., buildings with a similar behavior during an earthquake) is described by a probable vulnerability index, which varies between 0 and 1, and is independent from the hazard severity level. The ISTAT data allow to classify buildings into vulnerability classes (A to F) of the EMS by assigning a score of vulnerability. The classification procedure is consistent with a vulnerability assessment at national scale (Meroni et al. 2000) calibrated on more than 28,000 detailed vulnerability forms (Benedetti and Petrini, 1984). The adopted method proposed by Bernardini et al. (2008) describes a deterministic classification of groups of buildings defined on the ISTAT data; this proposal takes an additional parameter, namely the date of seismic classification of the territory, consistent with criteria suggested by the EMS, which introduced classes D, E, F for buildings constructed with criteria (progressively more severe) of anti-seismic design. The damage scale is expressed by self-explaining terms (few, many, most) describing the interaction between the vulnerability classes and the intensity. These terms can be expressed in fuzzy mode into numerical values of probability (damage probability matrix). We adopted the definitions proposed by Bernardini et al. (2007) for the quantification of terms in the damage probability matrix, obtaining a macroseismic vulnerability curve describing a random variable of D (from grade 1, slight, to grade 5, collapse), depending on the intensity degree and vulnerability index. The results point out on the grade D2 (moderate damage) and the grade D3 (substantial to heavy damage) of the EMS, where non-structural damages are predominant (Fig. 8) for the two different scenarios.

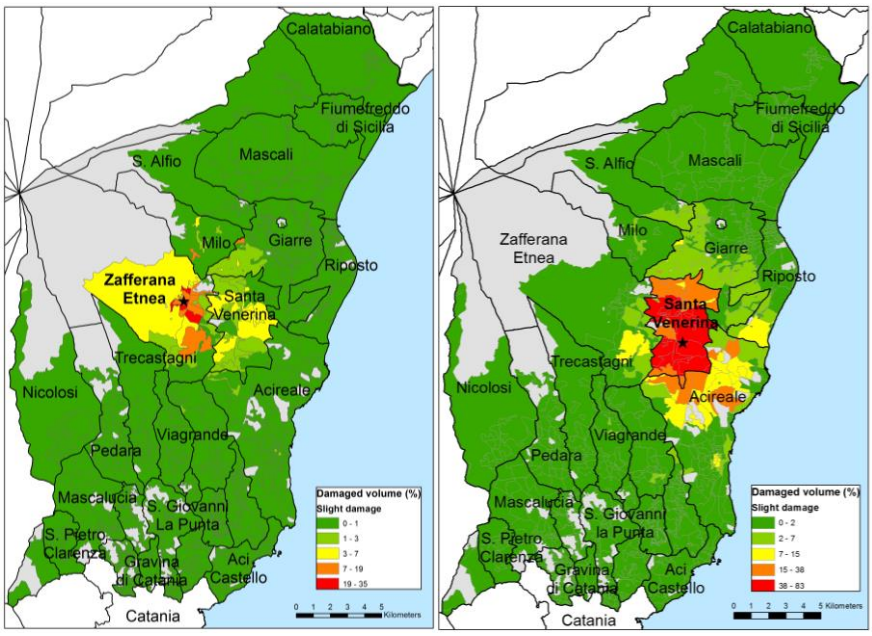

Figure 8. Slight damage (D1+D2+60%D3) calculated for each census sections of the municipalities for M_w 4.2 earthquake (left), and M_w 5.0 earthquake (right).

4.2 South Iceland Seismic Zone

The hazard scenario used for mapping the risk was taken as the larger ground motion produced by the two M_w 6.5 earthquakes of June 2000. The corresponding peak ground acceleration values were estimated from an equation presented in Rupakhety and Sigbjörnsson (2009). More details on the scenario hazard is presented in Bessason and Rupakhety (2018). Fragility curves for different building typologies were developed by Bessason and Bjarnason (2016); they are based on damage data collected after past earthquakes. For each building typology, damage states were defined as shown in Table 3.

Table 3. Definition of damage states for fragility curves of Icelandic residential buildings (damage factor is defined as estimated repair cost divided by replacement value).

Damage state	Range of damage factor	Description of damage
DS0	0%	No damage
DS1	>0 – 5%	Slight
DS2	>5 – 20%	Moderate
DS3	>20 – 50%	Substantial to heavy
DS4	>50%	Very heavy to total

Risk maps were computed and presented separately for different typologies. Risk was quantified in terms of probabilities of exceeding a damage state. Risk maps corresponding to DS1 for Reinforced Concrete (RC) buildings and built before and after 1980, are shown in Fig. 9. Similar maps were produced for other building types and damage states. As an example, the risk maps for Pre-1980 RC buildings show that in Selfoss, the probability of exceeding DS0 (no damage, not shown here) is in the range 0.10-0.20, while the probability of exceeding DS1 is less than 0.05.
The advantage of preparing separate risk maps for different typologies is that it avoids averaging over strong and weak buildings.

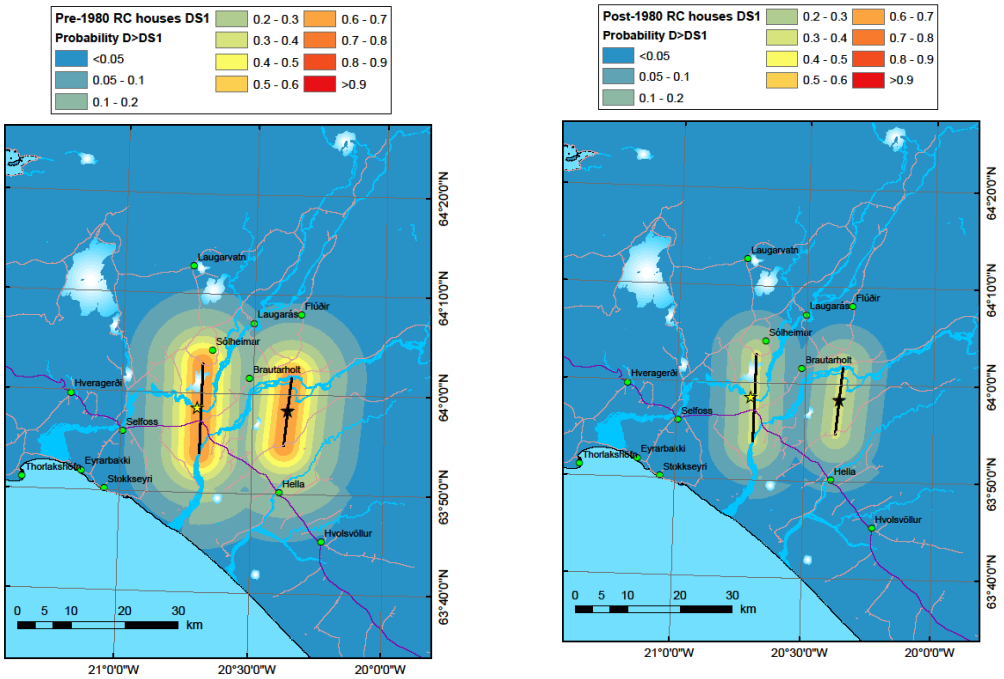

Figure 9. Scenario risk map for RC buildings built before and after 1980. The colors represent probability of exceeding DS1.

4.3 Lisbon, Portugal

In Lisbon a detailed RiskMAP was obtained the Alvalade parish, selected as pilot area. Alvalade is one of the 24 parishes of Lisbon municipalities and is characterized by a mix of urban uses (housing, commerce, services, schools, public spaces) and a socially diversified population. This community is composed by individuals: i) with a poor or no knowledge about Lisbon's seismic risk and about protection alternatives; ii) with perceptions based on beliefs that discourage the adoption of protective actions and which are poorly pro-active. So, providing simple guidelines for laypersons is one of the main objectives of project. Concerning graphic representation and arrangement for risk maps, an idealized map for the Lisbon pilot area could look like Fig. 10. Risk maps that depict the extent of non-structural damage expected after an earthquake, namely grades 2 and 3 as above defined, can provide basic information to be used effectively for community risk assessment and planning. In our approach, the map gives information on the average risk in each block, which is the smallest unit considered by the Census, and not building by building. It is therefore useful to raise awareness and for preparedness, but it cannot be directly used to decide which actions have to be undertook for each edifice. The following minimum requirements are important to compile the RiskMAP:
- identifying where people live with respect to the recognized hazard/risk;
- detecting important public buildings like schools and municipal buildings;
- having a small scale map that shows street names, building footprints in order to avoid questions like "where on this map is my home?"

These maps contain information not only about building damage expected after an earthquake, but also additional information/recommendations ("What should I do?").

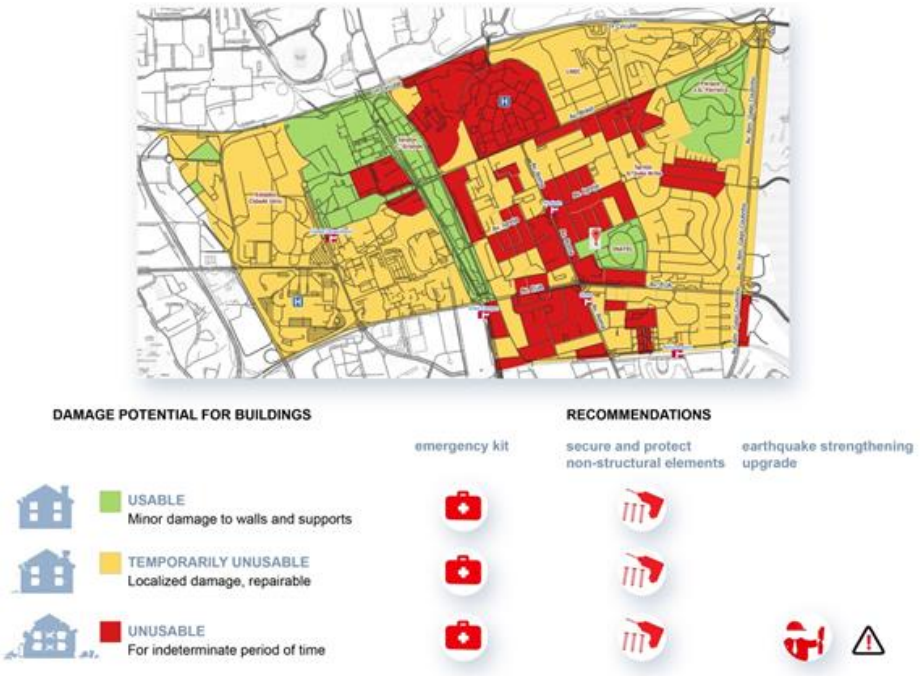

Figure 10. Expected pattern of building damage by block for an EC8 (Type II) scenario, and recommendations to reduce damage for the Alvalade pilot area. Estimates are based on the likelihood of damage in each of three states: slight (D1), moderate (D2-D3) and extensive (D4-D5).

5. CONCLUSIONS

In the three pilot areas different types of maps, with different scales (building by building, urban block, etc.) were developed, but we see that non-structural damage dominated the overall damage for all building typologies in the three countries. A new, important point is that vulnerability models using interstory drift as an intensity parameter, have not yet been developed, but there is a need for future

research to do so. Up to now there is no single format to communicate the non-structural risk to various types of end-users in different pilot areas, due to differences in seismicity, on data available for vulnerability characterization, level of risk culture and on the attitude of each regional expertise. How are maps to be designed to meet the particular requirements of communicating risk information to the authorities and the public? This paper presents variety of possible solutions and compromises among them. It is therefore necessary to continue the discussion on the format and scale of the risk maps for risk communication: should they show the risk for each building, for each typology, or the risk at local or regional level, should they show hazard or risk, considering the limitations of the available data. Some other indicator involving population affected could be considered.

6. ACKNOWLEDGMENTS

This study was co-financed by the European Commission's humanitarian aid and civil protection (grant agreement echo/sub/2015/718655/prev28). We are thankful for the discussions with all KnowRISK participants from the four institutions (IST, LNEC, INGV and EERC).

7. REFERENCES

Albarello D (2012). Design earthquake from site-oriented macroseismic hazard estimates. *Bollettino di Geofisica Teorica e Applicata*, 53(1): 7-18.

Azzaro R, D'Amico S, Rotondi R, Tuvè T, Zonno G (2013). Forecasting seismic scenarios on Etna volcano (Italy) through probabilistic intensity attenuation models: A Bayesian approach. *Journal of Volcanological and Geothermal Resarch*, 251: 149-157.

Azzaro R, D'Amico S, Tuvè T (2016). Seismic hazard assessment in the volcanic region of Mt. Etna (Italy): a probabilistic approach based on macroseismic data applied to volcano-tectonic seismicity. *Bulletin of Earthquake Engineering*, 14(7): 1813-1825, doi: 10.1007/s10518-015-9806-2.

Benedetti D, Petrini V (1984). On seismic vulnerability of masonry buildings: proposal of an evaluation procedure, *L'industria delle Costruzioni*, 18: 66-78.

Bernardini A, Giovinazzi S, Lagomarsino S, Parodi S (2007). Matrici di probabilità di danno implicite nella scala EMS98, *XII Convegno ANIDIS "L'ingegneria sismica in Italia"*, Pisa, Italy, CD-ROM.

Bernardini A, Salmaso L, Solari A (2008). Statistical evaluation of vulnerability and expected seismic damage of residential buildings in the Veneto-Friuli area (NE Italy). *Bollettino di Geofisica Teorica e Applicata*, 49(3-4): 427-446.

Bessason B, Bjarnasson J Ö (2016). Seismic vulnerability of low-rise residential buildings based on damage data from three earthquakes (Mw 6.5, 6.5, 6.3). *Engineering Structures*, 111:64-79.

Bessason B, Rupakhety R (2018). Seismic vulnerability of Icelandic residential buildings. In R. Rupakhety, S. Ólafsson (eds.), Earthquake Engineering and Structural Dynamics in Memory of Ragnar Sigbjörnsson, *Geotechnical, Geological and Earthquake Engineering*, 44, DOI 10.1007/978-3-319-62099-2_11.

Boore, DM (2009). Comparing stochastic point-source and finite-source ground-motion simulations: SMSIM and EXSIM. *Bulletin of Seismological Society of America*, 99: 3202–3216.

CMTE Working Group (2017). Catalogo Macrosismico dei Terremoti Etnei, 1600–2013. *Istituto Nazionale di Geofisica e Vulcanologia*, Catania. Italy, http://www.ct.ingv.it/macro/.

D'Amico V, Albarello D, Sigbjörnsson R, Rupakhety R (2016a). Seismic hazard assessment for Iceland in terms of macroseismic intensity using a site approach. *Bulletin of Earthquake Engineering*, 14:1797-1811.

D'Amico S, Meroni F, Sousa ML, Zonno G (2016b). Building vulnerability and seismic risk analysis in the urban area of Mt. Etna volcano (Italy). *Bulletin of Earthquake Engineering*, 14(7): 2031-2045.

Eurocódigo 8 (2010). Projecto de estruturas para resistência aos sismos, Parte 1: Regras gerais, acções sismicas e regras para edificios, *Anexo Nacional*, EC8 NP EN 1998-1.

Giardini D, Woessner J, Danciu L, Crowley H, Cotton F, Grunthal G, Pinho R, Valensise G, Akkar S, Arvidsson R, Basili R, Cameelbeeck T, Campos-Costa A, Douglas J, Demircioglu MB, Erdik M, Fonseca J, Glavatovic B,

Lindholm C, Makropoulos K, Meletti C, Musson R, Pitilakis K, Sesetyan K, Stromeyer D, Stucchi M, Rovida A (2013). Seismic hazard harmonization in Europe (SHARE): Online Data Resource. doi:10.12686/SED-00000001-SHARE

Giovinazzi S, Lagomarsino S (2001). Una metodologia per l'analisi di vulnerabilità sismica del costruito, *Proceedings of the X Congresso Nazionale "L'ingegneria Sismica in Italia"*, Potenza-Matera, Italy, CD-Rom.

Grünthal G, (eds.) (1998). European macroseismic scale 1998 (EMS-98). *European Seismological Commission, subcommission on Engineering Seismology, working Group Macroseismic Scales*. Conseil de l'Europe, Cahiers du Centre Européen de Géodynamique et de Séismologie 15, Luxembourg: pp 99. http://www.ecgs.lu/cahiers-bleus/.

Lagomarsino S, Giovinazzi S (2006). Macroseismic and mechanical models for the vulnerability and damage assessment of current buildings, *Bulletin of Earthquake Engineering*, 4: 415-443.

Langer H, Tusa G, Scarfì L, Azzaro R (2016). Ground-motion scenarios on Mt. Etna inferred from empirical relations and synthetic simulations. *Bulletin of Earthquake Engineering*, 14(7): 1917-1943, doi 10.1007/s10518-015-9823-1.

Meroni F, Petrini V, Zonno G (2000). Distribuzione nazionale della vulnerabilità media comunale. In Bernardini A (ed) *La vulnerabilità degli edifici*, CNR-GNDT, Roma, pp.105-131.

Miranda E, Akkar S (2006). Generalized Interstory Drift Spectrum. *Journal of Struct. Engi*, 840-852, doi: 10.1061/ASCE0733-94452006132:6840

Mota de Sá F (2016). Seismic Risk - New instruments for Analysis and Communication. *Ph.D Thesis*, Instituto Superior Técnico, University of Lisbon, Lisbon, Portugal.

Mota de Sá F, Ferreira MA, Oliveira CS (2016). QuakeIST® earthquake scenario simulator using interdependencies. *Bulletin of Earthquake Engineering*. 14(7): 2047-2067. doi: 10.1007/s10518-016-9884-9.

Portuguese Census Survey 2011. http://censos.ine.pt

Rotondi R, Varini E, Brambilla C (2016). Probabilistic modelling of macroseismic attenuation and forecast of damage scenarios. *Bulletin of Earthquake Engineering*, 14(7): 1777-1796, doi: 10.1007/s10518-015-9781-7.

Rupakhety R, Sigbjörnsson R, (2009). Ground-motion prediction equations (GMPEs) for inelastic response and structural behavior factors. *Bulletin of Earthquake Engineering*, 7(3):637–659.

Rupakhety R, Olafsson S, Sigbjörnsson R (2016). Damage to residential buildings in Hveragerði during the 2008 Ölfus Earthquake: simulated and surveyed results. *Bulletin of Earthquake Engineering*, 14(7):1945-1955

Scarfì L, Langer H, Garcia-Fernandez M, Jimenez JM (2016). Path effects and local elastic site amplification: two case studies on Mt Etna (Italy) and Vega Baja (SE Spain). *Bulletin of Earthquake Engineering*, 14(7): 2117-2127, doi 10.1007/s10518-016-9883-x.

Solnes J, Sigbjörnsson R, Eliasson J (2004). Probabilistic Seismic Hazard mapping of Iceland. *Proceedings of the 13th World Conference on Earthquake Engineering*, Vancouver, Canada.

Sousa ML (2006). Risco Sísmico em Portugal Continental, *Ph.D Thesis*, Instituto Superior Técnico, UTL, Lisbon, Portugal.

Sousa ML (2008) Annualized Economic and Human Earthquake Losses for the Portuguese Mainland, *Proceedings of the 14th World Conference on Earthquake Engineering*, Beijing, China.

Teves-Costa P, Senos ML (2000). Estimation of site effects using microtremro measurements and analytical modelling - application to the Lower Tagus Valley. *Proceedings of 12thWorld Conference on Earthquake Engineering*, Auckland, New Zealand, No.1250, pp 8.

Vilanova SP, Fonseca JFBD (2004). Seismic hazard impact of the Lower Tagus Valley Fault Zone (SW Iberia). *Journal of Seismology*, 8: 331–345.

Woessner J, Danciu L, Giardini D, Crowley H, Cotton F, Gru¨nthal G, Valensise G, Arvidsson R, Basili R, Demircioglu MB, Hiemer S, Meletti C, Musson R, Rovida A, Sesetyan K, Stucchi M, the SHARE consortium (2015). The 2013 European Seismic hazard model: key components and results. *Bulletin of Earthquake Engineering*, doi:10.1007/s10518-015-9795-1.

Zonno G, Rotondi R, Brambilla C (2009) Mining macroseismic fields to estimate the probability distribution of the intensity at site. *Bulletin of the Seismological Society of America*, 98(5): 2876-2892.